FEBS Letters

Cholesterol facilitates interactions between α-synuclein oligomers and charge-neutral membranes

Andreas van Maarschalkerweerd [a], Valeria Vetri [b],[*], Bente Vestergaard [a],[*]

[a] Department of Drug Design and Pharmacology, University of Copenhagen, Universitetsparken 2, DK-2100 Copenhagen, Denmark
[b] Dipartimento di Fisica e Chimica, Universitá di Palermo, Viale delle Scienze Ed. 18, 90128 Palermo, Italy

A B S T R A C T

Oligomeric species formed during α-synuclein fibrillation are suggested to be membrane-disrupting agents, and have been associated with cytotoxicity in Parkinson's disease. The majority of studies, however, have revealed that the effect of α-synuclein oligomers is only noticeable on systems composed of anionic lipids, while the more physiologically relevant zwitterionic lipids remain intact. We present experimental evidence for significant morphological changes in zwitterionic membranes containing cholesterol, induced by α-synuclein oligomers. Depending on the lipid composition, model membranes are either unperturbed, disrupt, or undergo dramatic morphological changes and segregate into structurally different components, which we visualize by 2-photon fluorescence microscopy and generalized polarization analysis using the fluorescent probe Laurdan. Our results highlight the crucial role of cholesterol for mediating interactions between physiologically relevant membranes and α-synuclein.

© 2015 Federation of European Biochemical Societies. Published by Elsevier B.V. All rights reserved.

1. Introduction

α-Synuclein (αSN) is an intrinsically disordered protein known to be implicated in Parkinson's disease (PD) etiology. A prominent hallmark of PD is the formation and deposition of cytosolic Lewy Bodies, with a characteristic rich content of lipids and fibrillated αSN [1–3]. Such protein fibrils are formed by complex and supramolecular assembly pathways. Several studies have suggested that intermediate species, rather than the fibril end-product, are the main toxic species and that interactions between amyloidogenic proteins and cell membranes are critical to the onset and progression of PD [4–7]. Accordingly, the unraveling of the molecular basis of such protein:membrane interactions may be the key to understand the link between in vivo amyloid formation and the inherent toxicity [8].

The structural and biophysical states of proteins and membranes are likely to be mutually dependent. Membrane physico-chemical and structural characteristics regulate the protein aggregation phenomena, and vice versa, which may result in either promoting or suppressing aggregation and modulating cellular response to oligomeric proteins [9,10]. Accordingly, studies of toxicity mediated by protein:membrane interactions should include observations of both lipid and protein structural and biophysical changes [11–13].

By such an approach, we have recently shown that αSN is able to induce disruption of anionic POPG vesicles, in a process including dehydration of the lipid bilayer, resulting in the formation of dense protein:lipid co-aggregates [13]. Various αSN oligomeric species have been reported to have membrane-disrupting effects on pure anionic phosphatidylglycol (PG) liposomes [14–17]. In contrast, the interaction between αSN and systems composed of neutral phosphatidylcholine lipids (PC) causes no significant effect [14–16]. Interestingly, interactions of amyloid-β oligomers and neutral membranes can be mediated by incorporation of cholesterol in the membranes [18]. This exemplifies the importance of varying lipid compositions in model systems, particularly including physiological-like compositions, when elucidating protein and membrane biochemical and biophysical properties [19–21].

Neuronal cell-membranes are characterized by a high content of neutral lipids and cholesterol [22]. Cholesterol plays a crucial role in regulating membrane structure, plasticity (inducing rigidity in the bilayer) and functional activity [23] and generally modulates amyloid protein interactions with lipids [14,18,24]. In the physiological membrane, cholesterol is present at high concentrations in specific liquid-ordered microdomains, which are thought to induce specific interaction with proteins and to be implicated in templating protein aggregation [22]. This highlights the importance of further investigations of the role of cholesterol-containing lipid bilayers in context of fibrillating proteins, which is the focus of the current study.

Different studies of the effect of αSN oligomers on model systems report seemingly conflicting results. Such recent results include variations in the reported potency of vesicle disruption for various types of oligomers [13,15,16]. It is very likely that the controversy of experimental results arises from finer differences in the experimental conditions applied in each study. During the fibrillation reaction, both on- and off-pathway species may be formed. Particularly stable off-pathway species may be isolated from the reaction mixtures [16], whereas on-pathway species are transient intermediates [13,15], only existing in equilibrium with native and/or fibril species. Such species can hence not be isolated from the mixtures. As a consequence, studies of the effect of purified species and mixtures are difficult to compare [17], although both types of studies are relevant.

This underlines the importance of investigating well-defined systems. If either the protein or the lipid components of the reaction mixture are poorly defined, observations can be difficult to interpret. In our previous studies we have used small-angle X-ray scattering (SAXS) to pre-characterize the protein species, prior to mixing with the model lipid systems [13]. Interestingly, a strategically designed small-molecule, the ring-fused 2-pyridone FN075 [25], induces the formation of and stabilizes αSN oligomers whose core-structure and overall dimensions are analogous to the on-pathway in-equilibrium oligomers [15,17,26]. The inclusion of FN075 hence enables the study of the effect of interaction between the membrane and a well-defined oligomeric state of αSN oligomers (FN-oligomers).

Our present analysis from such well-defined reaction mixtures reveal, quite unexpectedly, how the presence of cholesterol in neutral membranes drastically changes the effect of FN-oligomers. The overall effect on cholesterol-containing neutral lipid systems is distinct from that on anionic lipid systems. In the presence of cholesterol, FN-oligomers cause the formation of protein:lipid co-aggregates, as previously reported for anionic membranes [13] while the remaining membrane moiety exhibits a severely modulated morphology. In a cellular environment, such drastic effects would significantly alter cell functionality.

2. Materials and methods

2.1. FN-oligomer preparation

Recombinant αSN was expressed in *E. coli* BL21 (DE3) cells and purified as previously described [13]. FN075 was received as a kind gift from Almqvist [25]. αSN was dissolved in PBS buffer (20 mM phosphate, 150 mM NaCl at pH 7.4) and filtered with 0.22 μm centrifugal filter units (Millipore). FN-oligomers were prepared from native αSN stock solutions by adding FN075 in a 6:1 FN075:protein molar ratio followed by whirl mixing. The concentration of αSN and of FN075 stocks were determined using extinction coefficients of $5120 \, M^{-1} \, cm^{-1}$ [13] and $10,000 \, M^{-1} \, cm^{-1}$ [17], respectively.

2.2. Preparation of Laurdan stained liposomes

Lipids were purchased from Avanti Polar Lipids. Giant vesicles (GVs) were prepared from 1-hexadecanoyl-2-(9Z-octadecenoyl)-*sn*-glycero-3-phospho-(1′*rac*-glycerol) [POPG], 1-hexadecanoyl-2-(9Z-octadecenoyl)-*sn*-glycero-3-phosphocholine [POPC] and POPC:cholesterol [POPC:chol] in a 1:1 M ratio. The lipid stocks were prepared in chloroform and dried overnight in round flasks on a rotary evaporator. The dry lipid films were hydrated with 20 mM HEPES buffer (220 mM KCl, 0.06 mM $CaCl_2$, 0.02 mM EDTA, pH 7.4), mixed and then sonicated. The resulting lipid solutions were mixed on a whirl-mixer every 10 min for one hour and left for one more hour to anneal. GV samples were stained with Laurdan (Sigma Aldrich) according to standard protocols [27] and left to equilibrate for a minimum of 3 h before use. Laurdan:lipid molar ratio was 1:400.

2.3. Measurements of membrane biophysics in bulk

Changes of the mobility of water in the membrane were analyzed by means of Laurdan generalized polarization (GP) described by Parasassi et al. [28]. Fluorescence measurements of Laurdan stained GV samples at a lipid concentration of 400 μM were carried out on a Jasco FP-8500 equipped with a peltier-thermostat in semi-micro plastic cuvettes. Emission spectra were measured at 25 °C in the range 370–620 nm under excitation at $\lambda_{exc} = 375$ nm, (5 nm ex/em bandwidth, 1 s response time, 100 nm/min scan speed). FN-oligomers were added to the GVs in lipid:protein (*L/P*) molar ratios ranging from 20:1 to 100:1 and the fluorescent emission was recorded every 4 min after protein addition. The cuvettes were shaken gently prior to each measurement to keep the samples uniformly dispersed. The GP ratio of Laurdan was calculated according to Parasassi et al. [28]. Control measurements were performed to ensure that addition of buffers, DMSO or FN075 alone did not alter the stability of the liposomes. Additional control experiments are described elsewhere [13].

2.4. Measurements by 2-photon microscopy (2PM)

Laurdan stained GVs were deposited in Chambered Coverglass (Lab-Tek IINunc). 512×512 pixels image stacks were sequentially acquired using a Leica TCS SP5 confocal scanning microscope with a $63\times$ oil objective (Leica Microsystems, Germany). 2-Photon excitation was set at 780 nm (Spectra-Physics Mai-Tai Ti:Sa ultra-fast laser). Fluorescence signals were simultaneously recorded in two channels [13,29]: 410–460 nm (blue channel) and 480–540 nm (green channel). Data were acquired as a function of time before and after the addition of FN-oligomers. Images were cropped to 256×256 pixels prior to analysis with the SimFCS program (Laboratory for Fluorescence Dynamics, University of California, Irvine, CA), using either RICS screen or FRET screen of the program. Calibration of the GP scale to obtain a GP = 0.27 for a standard Laurdan solution in DMSO at 22 °C [29]. Control measurements have revealed that in our experimental conditions and in the absence of protein the samples, shape and morphology of observed liposomes do not change within the measurements of time interval and longer.

3. Results

In Fig. 1 we report spectroscopic measurements of changes in GP ratios as a function of time after FN-oligomer addition to POPG (Fig. 1A) and POPC:chol (Fig. 1B) GV bulk samples. GP reports the changes in Laurdan fluorescence spectra giving valuable information on the membrane structural and dynamical properties and in particular on the level of lipid packing and hydration
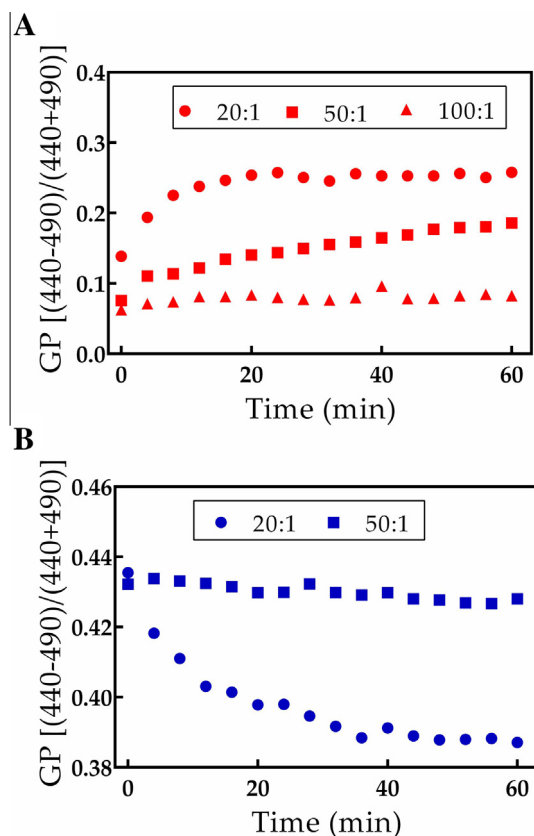
Fig. 1. Time evolution of GP ratios obtained from the analysis of Laurdan fluorescence spectrum variations, measured in bulk. (A) Time evolution of GP ratios calculated for POPG GV show an increase due to blue shifted fluorescent emission after addition of αSN FN-oligomers at *L/P* ratios of 20:1 (circles), 50:1 (squares) and 100:1 (triangles). (B)Time evolution of GP ratios calculated for POPC:chol GV show a decrease due to overall red shifted fluorescent emission after addition of αSN FN-oligomers at *L/P* ratios of 20:1 (circles) and 50:1 (squares).

[27,28,30–32]. Differences in the Laurdan spectrum have been ascribed to differences in water penetration into the membrane between the gel and liquid crystalline phases [30–32]. The results in Fig. 1A show a concentration dependent increase in GP ratios in anionic lipid samples. The changes toward higher GP values can be interpreted as indicative of progressive changes of membrane fluidity toward an ordered gel phase due to a progressive dehydration of the lipid bilayer [32]. These results are in line with previous results on POPG GV analyzed in analogous conditions with various αSN species, indicating that membrane disruption caused by reactive αSN species is coupled to an increased rigidity caused by dehydration of the membrane [13]. In line with previous results [13], FN-oligomers do not exert any effect on POPC GVs in the same experimental conditions (see Fig. S1).

Importantly, when αSN FN-oligomers are added to POPC:chol liposomes 1:1 (Fig. 1B) significant changes are revealed. The decrease in the GP ratio can be ascribed to changes in the membrane toward an increasingly disordered phase. Note that GP ratio variations for POPC:chol GV are of a lesser extent and in the opposite direction compared to those for POPG GVs, and also that the starting GP ratio of POPC:chol is much higher (i.e. a more rigid structure) than for POPG GVs. Due to their intrinsic ergodic nature these measurements provide averaged information on the protein: vesicle interaction and reveal that intrinsically different phenomena occur in the two systems.

Analysis of two-photon microscopy images on analogous samples allowed us to add topological information. This reveals that the changes in GP cover are critically different and, particularly

for the POPC:chol samples, spatially heterogeneous events. Fig. 2 shows 256 × 256 representative GP maps for POPG and POPC:chol liposomes as a function of time prior to (panel A and E) and after the addition of αSN FN-oligomers (panel B–D and panel F–H for POPG and POPC:chol liposomes respectively). Experiments were performed by adding FN-oligomers at *L/P* ratio 50:1 for POPG and *L/P* 20:1 for POPC:chol.

GP analysis of 2PM images allows for real time monitoring of the direct effect of lipid:protein interactions on membrane biophysics, integrity and morphology. Data in Fig. 2B–D reveal that after the addition of αSN FN-oligomers to POPG GVs, the liposomes are rapidly destroyed leading to a comprehensive depletion of the liposome population (Movie S1 in SI) combined with an increase of the number of diffuse pixels characterized by high GP values. The FN-oligomers, which have been shown to be on-pathway to fibrillation [17], thus have the same overall effect on POPG oligomers (although more potently), as native and partly aggregated αSN containing a low percentage of transient oligomers [13].

Data in panel F–H show that after the addition of FN-oligomers (*L/P* 20:1) POPC:chol GVs undergo critical morphological changes and structural reorganization as they change in shape, size and GP distribution (Movies S2 and S3 in SI). Complete depletion of POPC:chol GVs was never observed, also not at the relatively high *L/P* ratios used. It is evident from the high GP, that the overall structure of the POPC:chol GVs is more rigid than that of POPG GVs, and that the POPC-cholesterol distribution is natively homogeneous within resolution, as expected according to Dietrich et al. [33]. In line with bulk data (Fig. 1), the average value of GP for each image progressively decreases with respect to the initial GP measured before oligomers addition (Fig. 2E), which is clearly a result of non-homogenous events. The distribution of GP in POPC:cholGV is progressively heterogeneous leading to spatial separation of regions with different GP highlighted by blue and red pixels. Small objects appearing in the surrounding of liposomes are polydisperse in sizes and they are characterized by higher GP values compared to the large liposomes present in the sample at the end of the reaction.

In Fig. 3A and B we report the time evolution of the average value of GP calculated for each image after the addition of FN-oligomers. The observed changes are in line with the ones obtained in bulk experiments, hence revealing that microscopy measurements are representatives of the bulk processes. A deeper analysis of data in Fig. 2E–H reveal that the lowering of GP for POPC:chol GV is clearly coupled with the broadening of the distribution of GP values. Importantly, the reduction of the overall GP simultaneously with the increase in its distribution width was previously observed in live cell cultures upon extracellular addition of aggregating proteins [11].

In Fig. 4A and B we report GP histograms, coming from the same analysis as in Fig. 2, for POPC:chol GV before and after 29 min of incubation with αSN FN-oligomers (relative to GP maps in Fig. 2E and H respectively). In GP histograms it is possible to select pixels grouped under Gaussian curves, highlighted in red and green, these pixels will appear with the same color code in the GP maps.

Before protein addition, the GP histogram indicates a fairly homogeneous distribution of GP within the membrane. The GP histogram in panel 4A is well described by a single Gaussian component narrowly centered on the average GP = 0.44 as can be seen in panel (C) where all liposome membranes are colored green. As a result of protein:membrane interactions, the GP distribution is broadened so that it can be decomposed into at least two Gaussian components; one at high GP values (green) and one at low GP values (red). The green Gaussian component in panel 4B was chosen with the same width as the one in panel 4A and it is centered at GP 0.45. The analysis obtained for measurements at other time intervals after FN-oligomers addition are reported in Fig. S2.
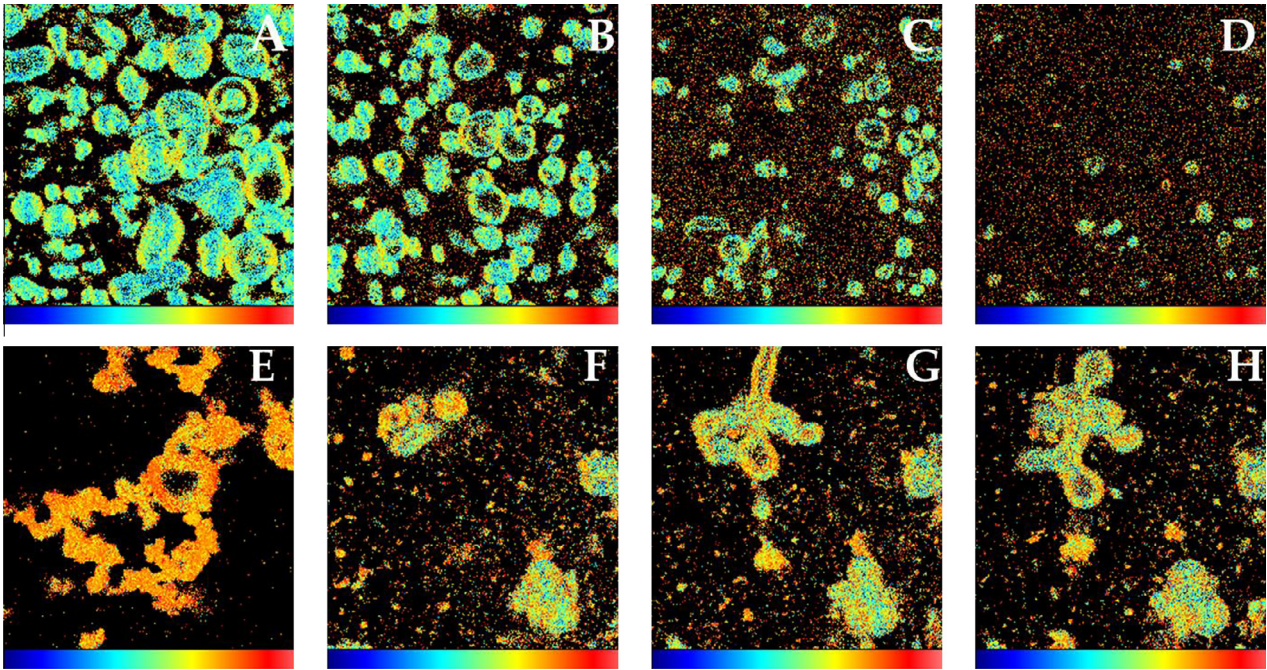
Fig. 2. Representative GP-image maps show distinct biophysical and morphological implications of lipid:protein interactions in POPG and POPC:chol GVs. POPG liposomes before (A) and 2 (B), 6 (C) and 11 min (D) after the addition of αSN FN-oligomers (*L/P* 50:1), clearly revealing liposome disintegration. POPC:chol liposomes before (E) and following 20 (F), 22 (G) and 29 min (H) of addition of αSN FN-oligomers (*L/P* 20:1) showing re-arrangements of liposome morphology. The color bars indicate the GP of each pixel ranging from −1 (blue) to +1 (red). The width of the images corresponds to 30 μm. Note the formation of an increased background (visible as red dots) over time for both POPG and POPC:chol samples.
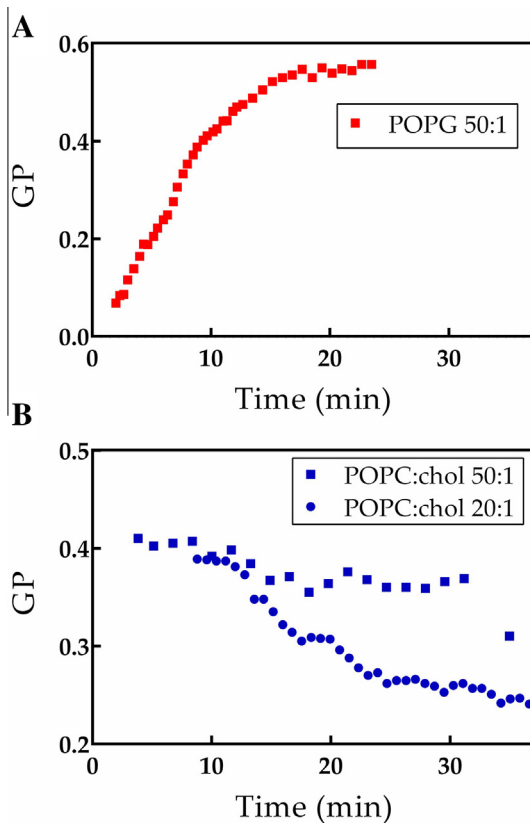

Fig. 3. GP values from 2PM as a function of time showing the GP increase in POPG (A) and the GP decrease in POPC:chol (B) following the addition of αSN FN-oligomers. *L/P* ratio 20:1 (circles) and *L/P* ratio 50:1 (squares).

The reported GP analysis drives the idea that spatially separated events occur in the sample driving critical modifications in POPC: chol GV which alter the mobility of water molecules in the membrane. It is evident that after incubation with FN-oligomers spatially separated domains with different GP values are formed, with higher GP values presumably being related to higher cholesterol content. Thus, it is possible to infer that the presence of FN-oligomers induces the formation of raft-like microdomains of discrete local concentrations of POPC and cholesterol.

Fig. 5 shows a representative image of POPC:chol GV after 45 min of incubation with FN-oligomers in the same experiment. The interaction with oligomers causes changes in the GP spatial distribution, and in the final state, it is possible to localize separated regions characterized by critically different GP values. We show representative selections of analyzed areas with different mean GP values including liposome regions with high (green square) and low GP values (blue square) as well as regions including small high GP value, which are appearing during incubation (red square). The liposomes have a severely altered overall morphology, but local regions display GP-histograms comparable to the histograms for non-modified membranes (green box in Fig. 5), while other regions reveal decreased GP (blue box in Fig. 5), i.e. increased flexibility in the membrane.

4. Discussion

The observations reported in this letter reveal that the interactions of FN-oligomers with lipid membranes result in different effects on membrane bilayers, depending on the lipid composition. We have analyzed model membranes containing cholesterol and POPC, which are among the major components of synaptic vesicles [22]. We compare the results to those for anionic phospholipid membranes. Pure anionic liposomes are often used as in vitro model systems as they mediate the electrostatic interactions
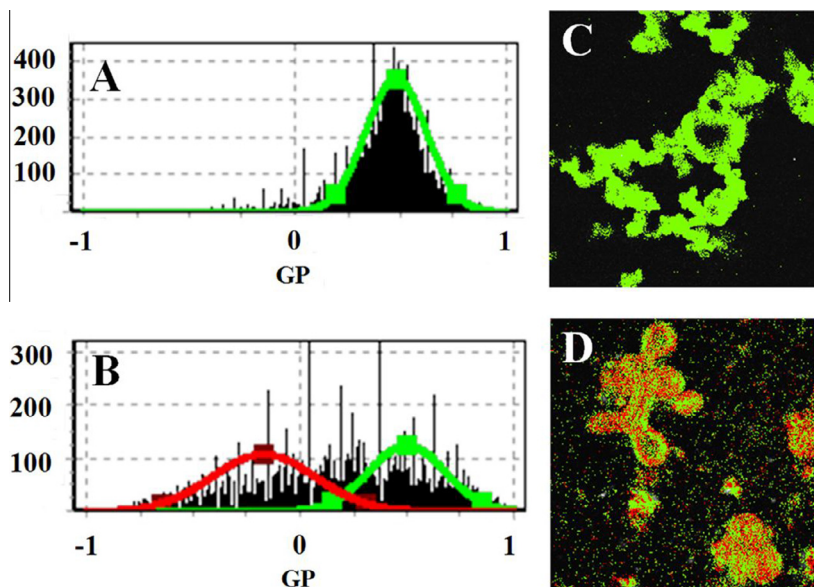
Fig. 4. GP histograms obtained from the analysis of POPC:chol liposomes sample before (A) and following 29 min (B) of the addition of FN-oligomers: the green and the red lines are used to select the Gaussian distributions of pixels with different average GP. It is possible to select these pixels in the corresponding binary maps (C, D). Colored points indicate pixels corresponding to the green and the red selections with the same color code.
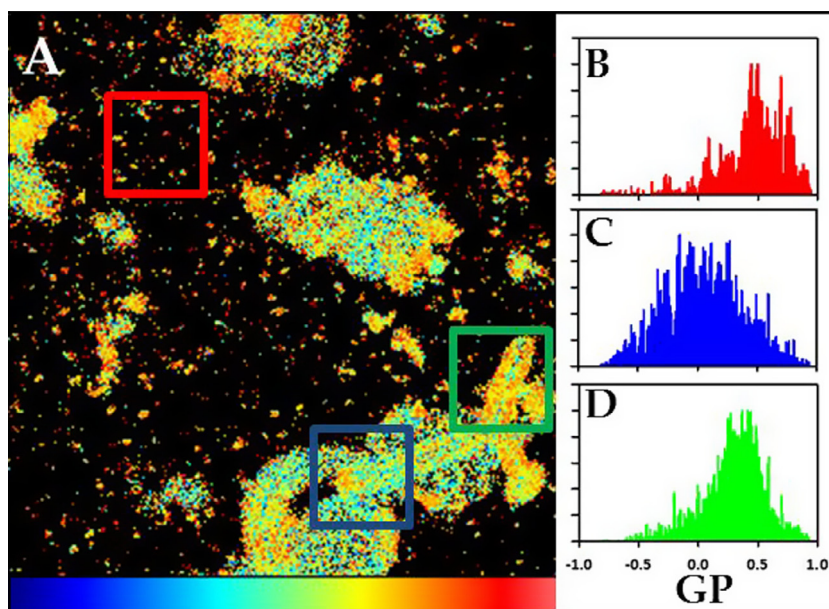

Fig. 5. Local variations of GP-distributions in modified liposomes observed with 2PM. The GP-map shows a POPC:chol structure 45 min after αSN-induced modification (*L*/*P* 20:1), characterized by regions of distinct local GP-distributions (lower right). Histograms in panel B, C and D are obtained from the analysis of 15 40 × 40 selections with analogous properties. The analysis was performed on areas where no intact liposomes are present (e.g. red square, average GP = 0.47) regions on intact liposomes were pixels with low GP are located (e.g. blue square, average GP = 0.02), regions on intact liposomes were pixels with high GP are located (green square, average GP = 0.39). It is possible to note that the average GP values of pixels in blue-like selections is close to the GP of single component POPC liposomes.

between membrane and proteins [34]. However, the anionic lipids are much less abundant than zwitterionic lipids in the membrane of synaptic vesicles [22].

Designing experimental studies of αSN oligomers is inherently challenging due to the unstable behavior of αSN oligomers outside their native environment. The use of chemically stabilized αSN oligomers provides an approach where well-defined on-pathway species can be studied undisturbed by the dynamics of ongoing fibrillation processes [17]. The high disruption potency of αSN FN-oligomers toward anionic membranes correlates well with

previous findings that identical [17] or related αSN oligomers [14–16] are able to induce substantial dye release from pure POPG and DOPG liposomes. The results presented here on the stabilized αSN oligomers thus highlight the effectiveness of this species in disturbing anionic membrane integrity. In accordance with previous reports [13–16] our experiments did not reveal any effects when FN-oligomers were added to single component POPC GVs. Moreover, we confirm existing results [18], supporting that dual-component POPC:chol membranes do interact with amyloidogenic oligomers. This is important since it emphasizes that

the FN-oligomer exhibits a behavior in accordance with other reports on αSN oligomers, and thus serves as a valid and well-defined model for the effect of on-pathway αSN fibrillogenic species [17].

It is not immediately evident how cholesterol facilitates the interaction between αSN FN-oligomers and vesicles. One effect may be found in the increased hydrophobicity in the bilayer, and modified electrostatic interactions in the membrane:solvent system [35]. Alternatively, the increased lipid head-group spacing mediated by cholesterol may facilitate protein interactions [14]. Finally, cholesterol is known to affect membrane flexibility by increasing the packing density of lipids [36–38] which we also observe by the high starting GP values for the POPC:chol GVs.

Most interestingly, our studies reveal several new lines of evidence. We reveal, firstly, that the net effect of αSN FN-oligomer addition to POPC:chol vesicles is a decrease in the bulk GP, which is opposite to that observed for anionic vesicles. Microscopy experiments give further details on the occurring mechanisms, revealing that two opposite effects occur. Firstly, FN-oligomers modify the structure of the POPC:chol membrane bilayer, causing the separation of regions with different GP in the resulting modified membrane morphology. The GP values and hence the density of the membrane structures vary greatly in the modified structures, suggesting that cholesterol no longer is uniformly distributed in the membrane structures which may potentially lead to a transition from liquid-order to a mixture of liquid-ordered and -disordered membrane [39]. Interestingly, the second overall observation is the simultaneous formation of smaller aggregates in the background, and these smaller species have increased GP-values (GP ≈ 0.4) (Fig. 2F–H). These objects may be cholesterol:protein co-aggregates, multicomponent structures including all three components, or maybe even pure cholesterol clusters although this last option seems unlikely.

It thus seems that the amyloidogenic protein oligomers while extracting lipid components and forming protein:lipid co-aggregates cause a partitioning of the cholesterol containing zwitterionic vesicles, thereby leaving a modified membrane structure with islands/rafts of varying ratios of POPC:chol. Such variations in the lipid composition will lead to local variations in membrane curvature, and hence result in the modified structures observed in this study (Fig. 2F–H). It is possible that similar effects in vivo would lead to significant variations in the membrane morphology or even membrane budding, and hence our observations could be related to the altered transport and exosomal activities reported in relation to PD disease progression [40]. The present data strongly suggest the occurrence of membrane compartmentalization and protein lipid co-aggregation this possibly having important biological implications. These data emphasize the need for further investigation into protein–lipid interactions and for characterization of physicochemical properties of co-aggregates. Others have shown, how changes in the equilibrium of phospholipid:sterol interactions after extraction of cholesterol from lipid bilayers cause the formation of segregated microdomains with high POPC content mainly in the disordered liquid phase [35]. Similar effects have been reported for amyloid precursor protein in Alzheimer's disease cell models, where cholesterol depletion altered membrane fluidity [41,42].

Our observations thus provide a model for how transiently formed amyloidogenic oligomers may cause a significant disturbance of the affected cells. If we extrapolate our results on the effect by the Parkinson's related αSN, this hence suggests that the neuronal membrane is modulated during disease progression, by interaction between specific lipid components and αSN oligomers, or a structural species co-existing with these oligomers [13]. If such αSN amyloidogenic species are able to extract and co-aggregate with particular lipids, this would result in significant membrane modulation, including curvature changes and varied membrane plasticity, thereby potentially causing alterations of both intra- and extra-cellular signaling, and thus ultimately disturbing the general machinery of the affected neurons.

Acknowledgements

Appendix A. Supplementary data

Supplementary data associated with this article can be found, in the online version, at http://dx.doi.org/10.1016/j.febslet.2015.08.013.

References

[1] Spillantini, M.G. et al. (1997) Alpha-synuclein in Lewy bodies. Nature 388 (6645), 839–840.

[2] Gai, W.P. et al. (2000) In situ and in vitro study of colocalization and segregation of α-synuclein, ubiquitin, and lipids in Lewy bodies. Exp. Neurol. 166 (2), 324–333.

[3] Gellermann, G.P. et al. (2005) Raft lipids as common components of human extracellular amyloid fibrils. Proc. Natl. Acad. Sci. U.S.A. 102 (18), 6297–6302.

[4] Butterfield, S.M. and Lashuel, H.A. (2010) Amyloidogenic protein–membrane interactions: mechanistic insight from model systems. Angew. Chem. Int. Ed. 49 (33), 5628–5654.

[5] Volles, M.J. et al. (2001) Vesicle permeabilization by protofibrillar α-synuclein: implications for the pathogenesis and treatment of Parkinson's disease. Biochemistry 40 (26), 7812–7819.

[6] Conway, K.A. et al. (2000) Acceleration of oligomerization, not fibrillization, is a shared property of both α-synuclein mutations linked to early-onset Parkinson's disease: implications for pathogenesis and therapy. Proc. Natl. Acad. Sci. 97 (2), 571–576.

[7] Winner, B. et al. (2011) In vivo demonstration that α-synuclein oligomers are toxic. Proc. Natl. Acad. Sci. 108 (10), 4194–4199.

[8] Straub, J.E. and Thirumalai, D. (2014) Membrane–protein interactions are key to understanding amyloid formation. J. Phys. Chem. Lett. 5 (3), 633–635.

[9] Bucciantini, M. et al. (2012) Toxic effects of amyloid fibrils on cell membranes: the importance of ganglioside GM1. FASEB J. 26 (2), 818–831.

[10] Evangelisti, E. et al. (2012) Membrane lipid composition and its physicochemical properties define cell vulnerability to aberrant protein oligomers. J. Cell Sci. 125 (10), 2416–2427.

[11] Vetri, V. et al. (2011) Fluctuation methods to study protein aggregation in live cells: concanavalin A oligomers formation. Biophys. J. 100 (3), 774–783.

[12] Stefani, M. (2010) Biochemical and biophysical features of both oligomer/fibril and cell membrane in amyloid cytotoxicity. FEBS J. 277 (22), 4602–4613.

[13] van Maarschalkerweerd, A., Vetri, V., Langkilde, A.E., Fodera, V. and Vestergaard, B. (2014) Protein/lipid coaggregates are formed during alpha-synuclein-induced disruption of lipid bilayers. Biomacromolecules 15 (10), 3643–3654.

[14] van Rooijen, B.D., Claessens, M.M. and Subramaniam, V. (2009) Lipid bilayer disruption by oligomeric alpha-synuclein depends on bilayer charge and accessibility of the hydrophobic core. Biochim. Biophys. Acta 1788 (6), 1271–1278.

[15] Giehm, L., Svergun, D.I., Otzen, D.E. and Vestergaard, B. (2011) Low-resolution structure of a vesicle disrupting alpha-synuclein oligomer that accumulates during fibrillation. Proc. Natl. Acad. Sci. U.S.A. 108 (8), 3246–3251.

[16] Lorenzen, N. et al. (2014) How epigallocatechin gallate can inhibit α-synuclein oligomer toxicity in vitro. J. Biol. Chem..

[17] Nors Perdersen, M. et al. (2015) Direct correlation between ligand-induced α-synuclein oligomers and amyloid-like fibril growth. Sci. Rep. 5.

[18] Ashley, R., Harroun, T., Hauss, T., Breen, K. and Bradshaw, J. (2006) Autoinsertion of soluble oligomers of Alzheimer's Abeta(1–42) peptide into cholesterol-containing membranes is accompanied by relocation of the sterol towards the bilayer surface. BMC Struct. Biol. 6 (1), 21.

[19] Fusco, G. et al. (2014) Direct observation of the three regions in alpha-synuclein that determine its membrane-bound behaviour. Nat. Commun. 5, 3827.

[20] Jiang, Z., de Messieres, M. and Lee, J.C. (2013) Membrane remodeling by α-synuclein and effects on amyloid formation. J. Am. Chem. Soc. 135 (43), 15970–15973.

[21] Stefanovic, A.N., Stockl, M.T., Claessens, M.M. and Subramaniam, V. (2014) Alpha-synuclein oligomers distinctively permeabilize complex model membranes. FEBS J. 281 (12), 2838–2850.

[22] Lim, L. and Wenk, M.R. (2010) Neuronal membrane lipids – their role in the synaptic vesicle cycle in: Handbook of Neurochemistry and Molecular Neurobiology (Lajtha, A., Tettamanti, G. and Goracci, G., Eds.), pp. 223–238, Springer, US.

[23] Liu, J.P. et al. (2010) Cholesterol involvement in the pathogenesis of neurodegenerative diseases. Mol. Cell. Neurosci. 43 (1), 33–42.

[24] Fantini, J. and Yahi, N. (2013) The driving force of alpha-synuclein insertion and amyloid channel formation in the plasma membrane of neural cells: key role of ganglioside- and cholesterol-binding domains. Adv. Exp. Med. Biol. 991, 15–26.

[25] Cegelski, L. et al. (2009) Small-molecule inhibitors target *Escherichia coli* amyloid biogenesis and biofilm formation. Nat. Chem. Biol. 5 (12), 913–919.

[26] Horvath, I. et al. (2013) Modulation of alpha-synuclein fibrillization by ring-fused 2-pyridones: templation and inhibition involve oligomers with different structure. Arch. Biochem. Biophys. 532 (2), 84–90.

[27] Sanchez, S.A., Tricerri, M.A., Gunter, G. and Gratton, E. (2007) Laurdan generalized polarization: from cuvette to microscope in: Modern Research and Educational Topics in Microscopy (Méndez-Vilas, A. and Díaz, J., Eds.), pp. 1007–1014, Springer, US.

[28] Parasassi, T., De Stasio, G., d'Ubaldo, A. and Gratton, E. (1990) Phase fluctuation in phospholipid membranes revealed by Laurdan fluorescence. Biophys. J. 57 (6), 1179–1186.

[29] Owen, D.M., Rentero, C., Magenau, A., Abu-Siniyeh, A. and Gaus, K. (2012) Quantitative imaging of membrane lipid order in cells and organisms. Nat. Protoc. 7 (1), 24–35.

[30] Parasassi, T. and Gratton, E. (1995) Membrane lipid domains and dynamics as detected by Laurdan fluorescence. J. Fluoresc. 5 (1), 59–69.

[31] Parasassi, T., Gratton, E., Yu, W.M., Wilson, P. and Levi, M. (1997) Two-photon fluorescence microscopy of laurdan generalized polarization domains in model and natural membranes. Biophys. J. 72 (6), 2413–2429.

[32] Parasassi, T. et al. (1994) Evidence for an increase in water concentration in bilayers after oxidative damage of phospholipids induced by ionizing radiation. Int. J. Radiat. Biol. 65 (3), 329–334.

[33] Dietrich, C. et al. (2001) Lipid rafts reconstituted in model membranes. Biophys. J. 80 (3), 1417–1428.

[34] Aisenbrey, C. et al. (2008) How is protein aggregation in amyloidogenic diseases modulated by biological membranes? Eur. Biophys. J. 37 (3), 247–255.

[35] Magarkar, A. et al. (2014) Cholesterol level affects surface charge of lipid membranes in saline solution. Sci. Rep. 4.

[36] Aguilar, L.F. et al. (2012) Differential dynamic and structural behavior of lipid-cholesterol domains in model membranes. PLoS ONE 7 (6), e40254.

[37] Sotomayor, C.P., Aguilar, L.F., Cuevas, F.J., Helms, M.K. and Jameson, D.M. (2000) Modulation of pig kidney Na^+/K^+-ATPase activity by cholesterol: role of hydration. Biochemistry 39 (35), 10928–10935.

[38] Fidorra, M., Duelund, L., Leidy, C., Simonsen, A.C. and Bagatolli, L.A. (2006) Absence of fluid-ordered/fluid-disordered phase coexistence in ceramide/POPC mixtures containing cholesterol. Biophys. J. 90 (12), 4437–4451.

[39] de Almeida, R.F., Fedorov, A. and Prieto, M. (2003) Sphingomyelin/phosphatidylcholine/cholesterol phase diagram: boundaries and composition of lipid rafts. Biophys. J. 85 (4), 2406–2416.

[40] Emmanouilidou, E. et al. (2010) Cell-produced α-synuclein is secreted in a calcium-dependent manner by exosomes and impacts neuronal survival. J. Neurosci. 30 (20), 6838–6851.

[41] Kojro, E., Gimpl, G., Lammich, S., März, W. and Fahrenholz, F. (2001) Low cholesterol stimulates the nonamyloidogenic pathway by its effect on the α-secretase ADAM 10. Proc. Natl. Acad. Sci. 98 (10), 5815–5820.

[42] von Arnim, C.A.F. et al. (2008) Impact of cholesterol level upon APP and BACE proximity and APP cleavage. Biochem. Biophys. Res. Commun. 370 (2), 207–212.